



^{99m}Tc production via the (γ, n) reaction on natural Mo

T. Takeda¹ · M. Fujiwara^{2,3} · M. Kurosawa² · N. Takahashi² · M. Tamura² · T. Kawabata¹ · Y. Fujikawa¹ · K. N. Suzuki¹ · N. Abe⁴ · T. Kubota⁴ · T. Takahashi⁴

Received: 1 March 2018 / Published online: 14 August 2018
© Akadémiai Kiadó, Budapest, Hungary 2018

Abstract

The worldwide supply of ^{99}Mo isotopes now encounters a serious crisis due to difficulties in sustainable production by research nuclear reactors. We report the experimental data for the ^{99m}Tc and impurity isotopes produced via the $^{nat}\text{Mo}(\gamma, n)$ reaction with bremsstrahlung γ -rays generated using a 30 MeV electron beam. The supply feasibility of ^{99m}Tc isotopes via the $^{nat}\text{Mo}(\gamma, n)$ reaction is discussed on the basis of the obtained data.

Keywords ^{99m}Tc , ^{nat}Mo , Mo and Nb impurities · Photoreaction · γ -decay measurements

Introduction

Soon after the discovery of artificially produced nucleus “Technetium” by Perrier and Segré [1, 2], the ^{99}Mo – ^{99m}Tc generator developed at Brookhaven National laboratory (BNL) [3] became an important imaging tool for medical diagnosis. The ^{99}Mo ground state with a half-life of $T_{1/2} = 66$ h decays to ^{99}Tc , and is trapped by the metastable 143 keV $1/2^-$ state in ^{99m}Tc with a half-life of 6 h. With an advantage of the long decay half-life, medical ^{99}Mo isotopes are exported to receiver hospitals using international flights. After arrival of ^{99}Mo isotopes, its daughter nuclide ^{99m}Tc is extracted several times by the milking method.

Huge amounts of $^{99}\text{Mo}/^{99m}\text{Tc}$ (more than 10^{16} Bq/year for 30 million patients in the world) are supplied from a limited number of the research nuclear reactors using highly enriched ^{235}U (HEU). The 6.1% ^{99}Mo fission yields

produced via the $^{235}\text{U}(n, f)$ reaction are processed to make ^{99}Mo solutions, which are shipped in the form of ^{99m}Tc milking generators. At receiver hospitals, the ^{99m}Tc radio-pharmaceuticals are used for Single-Photon Emission Computed Tomography (SPECT) inspections, giving great health-care benefits for patients. The ^{99}Mo supply system has worked stably in the past several decades. However, most of the research nuclear reactors used for ^{99}Mo production are now older than 45 years, and are operated over the period of durability. Serious concerns grow for safety problems due to aging, and for unscheduled shut-downs due to maintenance and repair work [4]. The research nuclear reactors with HEU tend to be shut down, because of the Partial Test Ban Treaty (PTBT) [5] and the Treaty on the Nonproliferation of Nuclear Weapons (NPT) [6]. In addition, many countries worry about the terrorism aiming at research nuclear reactors whose guard-defense is relatively weak [7].

In the last decade, alternative solutions have been searched for to establish a self-sufficiency system of $^{99}\text{Mo}/^{99m}\text{Tc}$ medical isotopes using particle accelerators by taking into account the scientific, political, and economical aspects [8]. Various kinds of nuclear reactions have been already studied and reviewed in Refs. [9–16]. When the ^{235}U and ^{238}U targets are used, we will be troubled by a problem in treating radioactive nuclear wastes like ^{239}Pu . When enriched Mo isotopes like ^{98}Mo and ^{100}Mo are employed, there remains a problem for expensive cost to buy the enriched isotopes used in a recycling loop. However, we do not exactly know the efficiency of recovering

✉ M. Fujiwara
fujiwara@rcnp.osaka-u.ac.jp

¹ Department of Physics, Kyoto University, Kitashirakawa-Oiwake, Sakyo, Kyoto 606-8502, Japan

² Research Center for Nuclear Physics, Osaka University, Mihogaoka 10-1, Ibaraki, Osaka 567-0047, Japan

³ National Institutes for Quantum and Radiological Science and Technology, Tokai, Ibaraki 319-1195, Japan

⁴ Institute for Integrated Radiation and Nuclear Science, Kyoto University, Kumatori, Osaka 590-0494, Japan

enriched isotopes in such a recycling loop. Even if the recovering efficiency of enriched isotopes is 95% [17, 18], we cannot use the expensive target material more than 50 times in the recycling loop since the enrichment of Mo materials is greatly reduced as $(0.95)^{50} = 0.07$ after the recycling process.

Direct ^{99m}Tc production via the $^{100}\text{Mo}(p, 2n)^{99m}\text{Tc}$ reaction has been discussed on a worldwide scale (for example, see Refs. [13, 14]). The direct ^{99m}Tc production at a cyclotron facility has been thought to be suitable for achieving a self-sufficiency system of ^{99m}Tc radio-pharmaceuticals. Although there are aforementioned disadvantages, the direct production of ^{99m}Tc radio-pharmaceuticals is attractive, and would become a good solution to make an in-house self-sufficiency system for a hospital with a positron emission tomography (PET) cyclotron, where medical doctors have a plenty of experience in treating ^{18}F radio-pharmaceuticals. However, a high-cost problem to import expensive enriched ^{100}Mo targets still remains. Since the range of a 20–30 MeV proton beam in a metallic molybdenum target is short as around 1 mm, the ^{100}Mo target used should be cooled down to avoid evaporation and melting due to a high energy–density deposit.

Nakai et al. [16] have proposed to make a self-sufficiency system of the ^{99}Mo – ^{99m}Tc isotopes by using various proton accelerators such as the J-PARC Linac injector, research cyclotrons, and PET cyclotrons in Japan. Advantages and disadvantages have been discussed in usage of these Japanese accelerators as a network system for stable supply of ^{99}Mo / ^{99m}Tc isotopes. Nakai et al. [16] conclude that about 300 TBq/year of ^{99}Mo isotopes will be available in the network of proton accelerator facilities. Since research nuclear reactors as well as accelerators often have routine shut-down for maintenance or repairing, the network system for stable supply of ^{99}Mo / ^{99m}Tc isotopes is inevitable.

Table 1 shows the half-lives and abundances of Nb, Mo and Tc isotopes relevant to the photoreactions on natural Mo targets. When the natural Mo target is irradiated by 20–30 MeV γ -rays, radioactive ^{90}Mo ($T_{1/2} = 5.67$ h) and ^{99}Mo ($T_{1/2} = 66$ h) isotopes are produced via the $^{92}\text{Mo}(\gamma, 2n)^{90}\text{Mo}$ and $^{100}\text{Mo}(\gamma, 2n)^{99}\text{Mo}$ reactions, respectively. The production of ^{93m}Mo isotopes with $T_{1/2} = 6.85$ h via (γ, n) reactions is expected to be extremely low, since the $J^\pi = 21/2^+$ high-spin state of ^{93m}Mo is not directly excited from the ^{94}Mo 0^+ ground state. It is noteworthy to mention that any Tc isotope other than ^{99m}Tc is not produced via the photoreactions on natural Mo isotopes. This is a great difference between the Tc isotope productions using charged particle reactions and photoreactions.

For example, if we use the nuclear reactions with a proton beam, impurity Tc isotopes other than ^{99m}Tc (such

as ^{94}Tc , ^{95}Tc , ^{96}Tc , and ^{97m}Tc) are easily produced via (p, n) and $(p, 2n)$ reactions on $^{\text{nat}}\text{Mo}$. Therefore, it is inevitable for us to use highly enriched and expensive ^{100}Mo isotopes for practical ^{99m}Tc productions in usage of a charged particle beam. Nb isotopes produced via (γ, p) or (γ, pn) reactions are obstacle impurities in preparing ^{99m}Tc radio-pharmaceuticals. These impurities should be reduced to be less than 10^{-4} to satisfy the specification requirement of the United States Pharmacopeial Convention [19]. The aforementioned impurity problem is solved by extracting only ^{99m}Tc isotopes in radiochemical procedures.

In the present paper, we report on the experimental measurements of the radioactivities produced via bremsstrahlung γ -ray irradiation on $^{\text{nat}}\text{MoO}_3$. On base of the present results, we wish to discuss whether or not the photo production of ^{99m}Tc on $^{\text{nat}}\text{Mo}$ can be incorporated in the worldwide supply system.

Bremsstrahlung γ -Ray Irradiation

We used a 30 MeV electron beam provided by the linear accelerator at Kyoto University Institute for Integrated Radiation and Nuclear Science (KURNS) [20]. The 30 MeV electron beam with an intensity of 17 μA bombarded a platinum target with a thickness of 4 mm for 3 min to generate bremsstrahlung γ -rays. The $^{\text{nat}}\text{MoO}_3$ powder with a weight of 0.5 g was encapsulated into a quartz tube with an inner diameter of 8 mm and an outer diameter of 10 mm. The distance between the 4 mm platinum target and the $^{\text{nat}}\text{MoO}_3$ powder target with a thickness of 4 cm was about 0.5 cm.

The bremsstrahlung γ -ray intensity on the target was estimated using the code G4beamline [22] developed on basis of Geant4 [23]. Figure 1 shows the bremsstrahlung γ -ray flux calculated under the assumption that a 30 MeV electron beam bombards a 4 mm platinum target. The threshold energies, $S_n = 8.29$ MeV, $S_p = 11.15$ MeV, $S_{2n} = 14.22$ MeV, and $S_{pn} = 18.03$ MeV for the $^{100}\text{Mo}(\gamma, n)$, $^{100}\text{Mo}(\gamma, p)$, $^{100}\text{Mo}(\gamma, 2n)$, and $^{100}\text{Mo}(\gamma, pn)$ reactions, respectively, are indicated in Fig. 1.

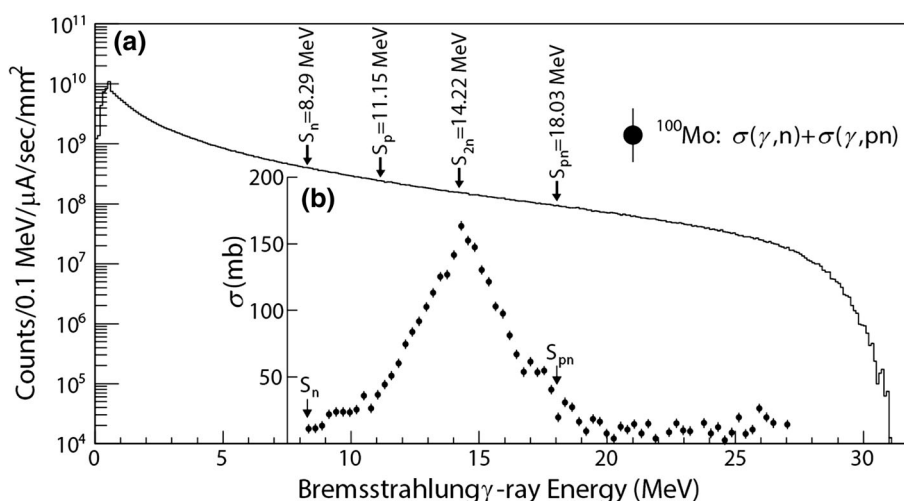
The (γ, n) reaction cross sections on Mo isotopes have been studied in detail as a function of the γ -ray energy, E_γ , by Beil et al. [24]. In case of the $^{100}\text{Mo}(\gamma, n)^{99}\text{Mo}$ reaction, the cross section has a broad peak at $E_\gamma = 14$ MeV with a width of 4 MeV. The integrated cross section of the $^{100}\text{Mo}(\gamma, n)^{99}\text{Mo}$ reaction over the energy range of 8–18 MeV amounts to about 1.0 MeV·b. This large cross section mainly comes from excitation of the giant dipole resonance (GDR) originated from the collective dipole vibration of protons against neutrons in nuclei.

Table 1 Half-lives of Nb, Mo, and Tc isotopes relevant to the ^{99m}Tc production. Listed are Mo, Tc and Nb isotopes with a half-life longer than 10 min and shorter than 100 days. The natural abundances of stable Mo isotopes other than ^{99m}Tc are not produced via photo production, irrelevant Tc isotopes such as ^{93}Tc , ^{94}Tc , ^{95}Tc , ^{96}Tc , and ^{97m}Tc are not listed

Niobium	Half-life	Molybdenum	Half-life (abundance)	Technetium	Half-life
^{90}Nb	14.6 h	^{90}Mo	5.67 h		
^{91m}Nb	61 days	^{91}Mo	15.5 m		
^{92m}Nb	10.2 days	^{92}Mo	(14.5%)		
		$^{93m}\text{Mo}^1$	6.85 h		
		^{94}Mo	(9.25%)		
^{95m}Nb	87 h	^{95}Mo	(15.92%)		
			(16.68%)		
^{96}Nb	23 h	^{96}Mo	(9.56%)		
^{97}Nb	72 m	^{97}Mo	(24.13%)		
		^{99}Mo	66 h	^{99m}Tc	6 h
		^{100}Mo	(9.63%)		

¹The half-life of the ^{93}Mo ground state is 4000 years. At the excitation energy of $E_x = 2572$ keV, there exists a metastable isotope, ^{93m}Mo , with a half-life of 6.85 h and a spin-parity of $21/2^+$. This metastable ^{93m}Mo decays to the ^{93}Mo ground state by IT transitions

Fig. 1 (a) Bremsstrahlung γ -ray flux generated by a 30 MeV electron beam on a 4 mm platinum metallic target. The threshold energies for the (γ, n) , (γ, p) , $(\gamma, 2n)$, (γ, pn) reactions on ^{100}Mo are indicated. (b) The cross sections for the $^{100}\text{Mo}(\gamma, n) + (\gamma, pn)$ reactions are shown as a function of γ -ray energy



Decay γ -Ray Measurement

After bremsstrahlung γ -ray irradiation, the radioactive $^{\text{nat}}\text{MoO}_3$ powder in the quartz tube was set in front of the head surface of a 30% HPGe detector with a distance of 14 cm, and the γ -ray measurement was started in 100 min subsequent to the end of bombardment (EOB). The measurements of decay γ -rays from the irradiated MoO_3 powder were repeated in steps of 1 h elapsed time, and γ -ray energy spectra were stored as digital data. This process was repeated 140 times. The energy dependence of the γ -ray detection efficiency was calibrated using several standard sources like ^{57}Co , ^{60}Co , ^{85}Sr , ^{88}Y , ^{113}Sn , ^{137}Cs , ^{139}Ce , and ^{203}Hg .

Figure 2 shows the measured γ -ray spectra at the elapsed times of 24 h and 140 h after EOB. Characteristic strong peaks for 141 keV γ -rays due to the ^{99m}Tc decay have been clearly observed. Both the spectra show the γ -ray peaks at $E_\gamma = 181, 366, 740,$ and 778 keV due to the decays from the excited states in ^{99}Tc after the $^{99}\text{Mo} \rightarrow ^{99}\text{Tc}$ β -decay. Although the peaks at 822 keV and 960 keV were reported to be due to the ^{99}Mo decay in Ref. [21], their identifications was difficult in the present work because of relatively high backgrounds from impurity Nb radioisotopes. Other observed γ -ray peaks are due to the ^{90}Nb , ^{90}Mo , ^{91}Mo , ^{95}Nb , ^{95m}Nb , ^{96}Nb radioisotopes.

Figure 3 shows the decay curve of ^{99m}Tc obtained from the measurement of the 141 keV γ -ray yields. A typical shape for transient equilibrium is observed in case of the

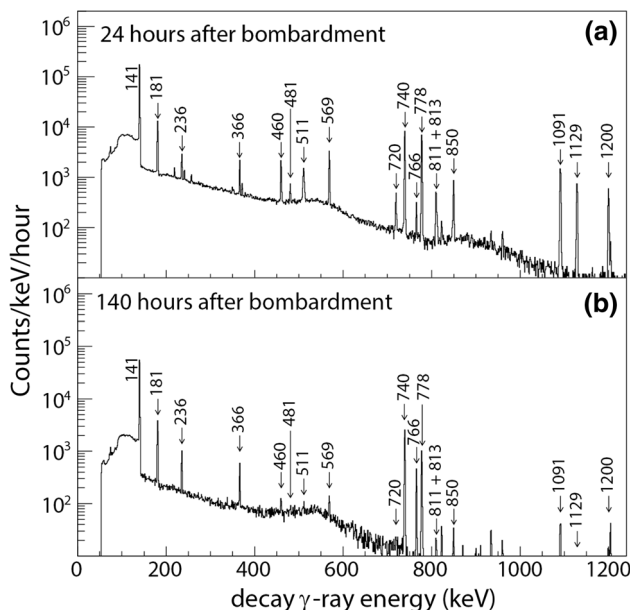


Fig. 2 Decay γ -ray spectra measured for 1-h data-taking time by a 30% HPGe detector. Two γ -ray spectra are shown at the elapsed times of **a** 24 h and **b** 140 h after EOB

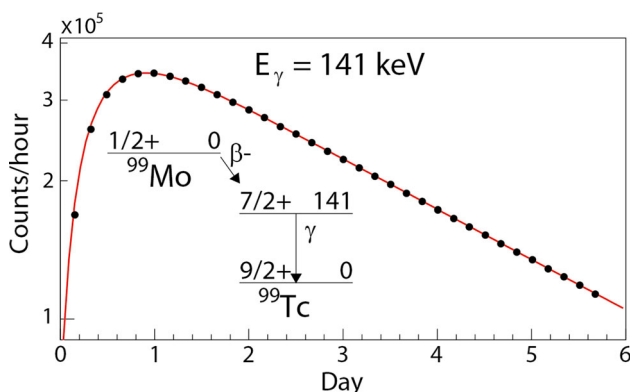


Fig. 3 The decay curve of ^{99m}Tc obtained from the 141 keV γ -ray measurement as a function of elapsed time. The partial decay scheme from the ^{99}Mo ground state to the ^{99}Tc ground state is illustrated. The solid curve is the result of data fitting with the transient-equilibrium equation

sequential decay from the ^{99}Mo ground state to the ^{99}Tc ground state through the metastable 143 keV excited state in ^{99}Tc . The activity yields Y_{Tc} of the daughter ^{99m}Tc is given by the following equation,

$$Y_{\text{Tc}}(t) = \left[Y_{\text{Mo}}(0) \frac{\lambda_{\text{Tc}}}{\lambda_{\text{Tc}} - \lambda_{\text{Mo}}} \times (e^{-\lambda_{\text{Mo}}t} - e^{-\lambda_{\text{Tc}}t}) \right] \times \text{BR} + Y_{\text{Tc}}(0)e^{-\lambda_{\text{Tc}}t}, \tag{1}$$

where Y_{Mo} is the activity of ^{99}Mo . λ_{Mo} and λ_{Tc} are defined as $\lambda_{\text{Mo}} = \log(2)/T_{1/2}(^{99}\text{Mo})$, and $\lambda_{\text{Tc}} = \log(2)/T_{1/2}(^{99m}\text{Tc})$, respectively. The parameter BR is the decay

branching ratio from the parent ^{99}Mo to the daughter ^{99m}Tc , which is 0.886. In case of ^{99}Mo – ^{99m}Tc generator, the maximum of the daughter yield is expected to be at the elapsed time of 24 h. As shown in Fig. 3, the experimental data are quite well reproduced using the equation for transient equilibrium. In good agreement with the theoretical expectation for transient equilibrium, the 141 keV γ -ray yield peaks at the elapsed time of one day after EOB.

By taking into account the electron beam current, bremsstrahlung photon yields, irradiation time, target mass of $^{\text{nat}}\text{MoO}_3$ and the γ -ray detection efficiency of the used HPGe detector including the geometrical effect, the ^{99m}Tc activity at the elapsed time of 24 h has been estimated to be $(7.4 \pm 0.9) \times 10^4$ Bq/ $\mu\text{Ah/g-MoO}_3$. We obtained the amount of the ^{99}Mo radioactivities by fitting the experimental data with the transient equilibrium curve for the ^{99m}Tc decay (see Fig. 3). The result is $(1.05 \pm 0.06) \times 10^5$ Bq/ $\mu\text{Ah/g-MoO}_3$. We confirmed that this result was consistent with those obtained from the decay rates of γ -rays at $E_\gamma = 181, 366, 740,$ and 778 keV due to the $^{99}\text{Mo} \rightarrow ^{99}\text{Tc}$ β -decay, although it was necessary for us to correct for each γ -ray branching-ratio. Note that using the production rate of $(1.05 \pm 0.06) \times 10^5$ - Bq/ $\mu\text{Ah/g-MoO}_3$, we can estimate the practical yields for the ^{99m}Tc production by taking into account the $^{\text{nat}}\text{MoO}_3$ target thickness, the $^{\text{nat}}\text{MoO}_3$ target size, the distance between the Pt bremsstrahlung target and the $^{\text{nat}}\text{MoO}_3$ target. Concerning this practical ^{99m}Tc yields, we will discuss more details later in the discussion section.

Figure 4 shows the decay curves of typical γ -rays observed in the present experiment. As shown in Fig. 4, almost all the decay data has been fitted by using the well-known half-life parameters. In case of the 766 keV γ -ray peak, the yields increase with increasing the elapsed time (see Fig. 4d). This behavior of the decay curve is well fitted using the transient-equilibrium equation, and we have reached at the conclusion that the 766 keV γ -ray peak is due to the decay chain of $^{95m}\text{Nb}(236 \text{ keV})$ ($T_{1/2} = 3.6$ days) \rightarrow $^{95}\text{Nb}(\text{g.s.})$ ($T_{1/2} = 35$ days) \rightarrow $^{95}\text{Mo}(766 \text{ keV})$.

Figure 5 shows the γ -ray spectrum measured at the elapsed time of 2 h after EOB. We observe tiny peaks due to γ -decays from ^{90}Mo ($T_{1/2} = 5.7$ h), ^{90}Nb ($T_{1/2} = 14.6$ h), ^{91m}Nb ($T_{1/2} = 61$ days), ^{92m}Nb ($T_{1/2} = 10$ days), ^{95}Nb ($T_{1/2} = 3.6$ days), ^{95m}Nb ($T_{1/2} = 35$ days), ^{96}Nb ($T_{1/2} = 23.35$ h), ^{97}Nb ($T_{1/2} = 72.1$ m), and ^{98m}Nb ($T_{1/2} = 51$ m).

By analyzing the γ -ray decay-curves for a period of relatively short-elapsed time, we have obtained the following conclusions:

1. The 122 keV and 257 keV γ -rays are attributed to the decays of ^{90}Mo ($T_{1/2} = 5.7$ h) produced via the $^{92}\text{Mo}(\gamma, 2n)$ reaction.

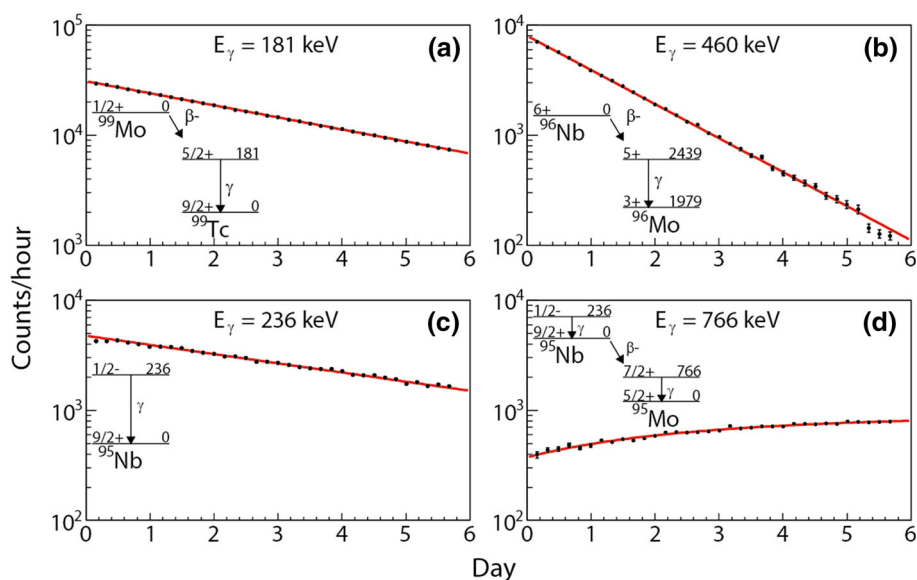
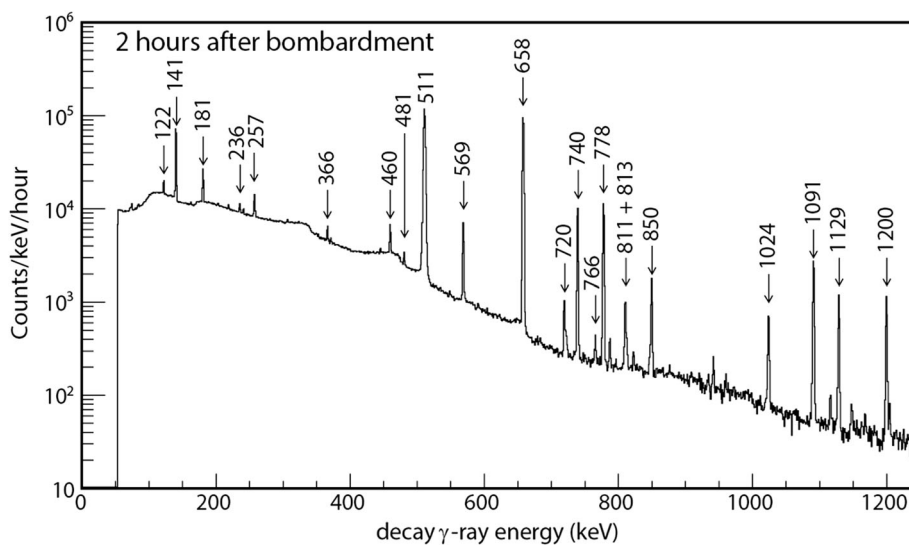


Fig. 4 Decay curves of typical γ -rays observed in the present experiment. The γ intensities are plotted as a function of elapsed time. The decay schemes are indicated for **a** $E_\gamma = 181$ keV from the β^- decay of ^{99}Mo ($T_{1/2} = 66$ h), **b** $E_\gamma = 460$ keV from the β^- decay

of ^{96}Nb ($T_{1/2} = 23$ h), **c** $E_\gamma = 236$ keV from the γ decay of $^{95\text{m}}\text{Nb}$ ($T_{1/2} = 3.6$ d), **d** $E_\gamma = 766$ keV from the decay chain of $^{95\text{m}}\text{Nb}$ (236 keV) ($T_{1/2} = 3.6$ days) \rightarrow $^{95}\text{Nb(g.s.)}$ ($T_{1/2} = 35$ days) \rightarrow ^{95}Mo (766 keV), respectively

Fig. 5 Decay γ -ray spectra measured at the elapsed time of 2 h after EOB. The setup of the measurement is the same as explained in the caption of Fig. 2



- The 1129 keV and 2319 keV γ -rays are due to the decay chain of $^{90}\text{Mo} \rightarrow ^{90}\text{Nb} \rightarrow ^{90}\text{Zr}$. The decay curves of the 1129 keV and 2319 keV γ -rays are well fitted by using the transient-equilibrium equation with ^{90}Mo ($T_{1/2} = 5.7$ h) and ^{90}Nb ($T_{1/2} = 14.6$ h). The activities obtained from both the 1129 keV and 2319 keV γ -ray intensities are in agreement with $(1.7 \pm 0.1) \times 10^3$ Bq/ $\mu\text{Ah/g-MoO}_3$ at the elapsed time of $t = 0$ after making the correction for the decay branching ratio.
- The 1204 keV γ -ray peak is observed in energy above the 1200 keV γ -ray peak due to the ^{96}Nb decay. Since

the half-life of the $^{91\text{m}}\text{Nb}$ is long as 61 days, and since the 1204 keV peak intensity is weak, we have not obtained the decay yields of $^{91\text{m}}\text{Nb}$ at $t = 0$ because of high backgrounds (see “[Final remarks and conclusion](#)” section for the estimation for these weak γ -decay yields).

- On base of the decay curve of 511 keV γ -rays, we conclude that there is evidence for the ^{91}Mo production via the $^{92}\text{Mo}(\gamma, 2n)$ reaction. Because of the short half-life ($T_{1/2} = 15.5$ m) of ^{91}Mo , we could not obtain the activity yields at $t = 0$.
- The production of $^{92\text{m}}\text{Nb}$ ($T_{1/2} = 10.2$ days) is identified from the γ -ray peak at 934 keV. The 934 keV

peak has been clearly observed in the spectra at the elapsed time of $t \geq 100$ h although the peak yields are weak (see “Final remarks and conclusion” section for the estimation for these weak γ -decay yields).

6. The spin and parity J^π of the ^{95}Nb ($T_{1/2} = 35$ days) ground state is $9/2^+$. Therefore, it is difficult to directly produce the ^{95}Nb ground state via the $^{96}\text{Mo}(\gamma, p)$ reaction. In the (γ, p) reaction, the Giant Dipole Resonance (GDR) with $J^\pi = 1^-$ is excited by photon absorption, and secondly one proton is emitted from the GDR. In order to make the final $J^\pi = 9/2^+$ state in ^{95}Nb , emitted proton has to carry the transferred angular momentum $L = 5$. This probability is extremely small. On the other hand, there is a metastable state with $J^\pi = 1/2^-$ at $E_x = 236$ keV in ^{95}Nb . This state can be possibly produced via the $^{96}\text{Mo}(\gamma, p)$ reaction. We have observed the γ -ray peaks at 236 keV and 766 keV from the sequential decay of $^{95\text{m}}\text{Nb} \rightarrow ^{95}\text{Nb}(\text{g.s.}) \rightarrow ^{95}\text{Mo}$. The decay curve for the 236 keV peak is well described with the known half-life of $T_{1/2} = 3.6$ days. The decay curve of the 766 keV peak has been fitted well using the transient-equilibrium equation.
7. The γ -ray peaks at $E_\gamma = 219, 241, 460, 481, 569, 720, 778, 811, 813, 850, 1091, 1200, 1498$ keV are found to be attributed to the decay from ^{96}Nb to ^{96}Mo . All the decay curves for these γ -ray peaks are well fitted with the half-life of $T_{1/2} = 23$ h. Taking into account the decay branching ratios and the detection efficiencies for these γ -rays, we have obtained the ^{96}Nb activity of $(10.8 \pm 0.4) \times 10^3$ Bq/ $\mu\text{Ah/g-MoO}_3$ at $t = 0$, which are constant, irrespective of γ -ray energy.
8. The γ -rays associated with the decay of ^{97}Nb have been observed at $E_\gamma = 658, 1024, 1117$ keV. The spin and parity J^π of the ^{97}Nb ground state ($T_{1/2} = 72$ m) is $9/2^+$. Thus, the ^{97}Nb ground state is not directly fed via the $^{98}\text{Mo}(\gamma, p)$ reaction. However, the ^{97}Nb ground state is produced as a short trapping state through the giant dipole resonance (GDR) excitation as a doorway state with $J^\pi = 1/2^-$ in ^{97}Nb from ^{98}Mo with $J^\pi = 0^+$. The experimental decay curves for the peaks at $E_\gamma = 658, 1024, 1117$ keV are in good agreement with those obtained under the assumption of a half-life of $T_{1/2} = 72$ m. The radioactivity yield at $t = 0$ becomes $(3.9 \pm 0.4) \times 10^5$ Bq/ $\mu\text{Ah/g-MoO}_3$, which is the averaged value for the measured γ -ray yields obtained by analyzing the 658, 1024, 1117 keV peaks.
9. We have observed a tiny 787 keV peak at the high energy side of the 778 keV peak (see Fig. 5). The decay curve of the 787 keV γ -ray is well fitted with the half-life $T_{1/2} = 51$ m of $^{98\text{m}}\text{Nb}$ (5^+). This metastable state is inferred to be excited through the

GDR excitation via the $^{100}\text{Mo}(\gamma, pn)$ reaction. However, it is not clear for us to correctly understand the reason why $^{98\text{m}}\text{Nb}$ with $J^\pi = 5^+$ is excited via photo absorption. This problem remains unsolved. The $^{98\text{m}}\text{Nb}$ radioactivity is $(2.5 \pm 0.5) \times 10^3$ Bq/ $\mu\text{Ah/g-MoO}_3$ at the elapsed time of $t = 0$, and is very small at $t = 24$ h.

Discussion

Table 2 summarizes the radioactivities produced by irradiating the bremsstrahlung γ -ray beam on a $^{\text{nat}}\text{MoO}_3$ target. In Table 2, normalized radioactivities of observed nuclei are given at the elapsed times of $t = 0$ and $t = 24$ h after the 3 min irradiation of bremsstrahlung γ -ray beam. The radioactivities at $t = 24$ h are obtained using simple decay calculations and transient equilibrium calculations with the known half-life of produced each nucleus.

The reasons why we have difficulties in determining the reliable amounts of the ^{90}Mo , $^{91\text{m}}\text{Nb}$, ^{91}Mo and $^{92\text{m}}\text{Nb}$ radioactivities in the present experiment are discussed in more detail as follows;

1. We have identified that the ^{90}Mo isotopes are produced via the $^{92}\text{Mo}(\gamma, 2n)$ reaction with the threshold value of $S_{2n} = 22.8$ MeV [24]. The 122 keV and 257 keV γ -rays are attributed to the decays of ^{90}Mo ($T_{1/2} = 5.7$ h). The 1129 keV and 2319 keV γ -rays are due to the decay chain of $^{90}\text{Mo} \rightarrow ^{90}\text{Nb} \rightarrow ^{90}\text{Zr}$. The decay curves of these two γ -rays are well fitted using the transient-equilibrium equation with ^{90}Mo ($T_{1/2} = 5.7$ h) and ^{90}Nb ($T_{1/2} = 14.6$ h). From the decay curve of the 1129 keV and 2319 keV γ -rays, we determined the amounts of the ^{90}Nb activities to be $(1.7 \pm 0.1) \times 10^3$ Bq/ $\mu\text{Ah/g-MoO}_3$ at $t = 0$ and $(1.3 \pm 0.2) \times 10^3$ Bq/ $\mu\text{Ah/g-MoO}_3$ at $t = 24$ h, respectively. It is inferred that the ^{90}Mo radioactivity is $(1.7 \pm 0.1) \times 10^3$ Bq/ $\mu\text{Ah/g-MoO}_3$ at $t = 0$, and is $(9.0 \pm 0.5) \times 10^1$ Bq/ $\mu\text{Ah/g-MoO}_3$ at $t = 24$ h.
2. The 1204 keV peak was identified to be due to the $^{91\text{m}}\text{Nb}$ decay. This 1204 keV peak appears as a shoulder part of the strong 1200 keV peak due to ^{96}Nb decay with $T_{1/2} = 23$ h (see Figs. 2, 5). Since the $^{91\text{m}}\text{Nb}$ half-life of $T_{1/2} = 61$ days is long, and since the background level of the γ -ray spectra soon after EOB is high, we could not reliably obtain the radioactivity yields at $t = 0$. It is noted that the yields of $^{91\text{m}}\text{Nb}$ are compatible with those of $^{92\text{m}}\text{Nb}$. We roughly estimated the yields to be less than 8.0×10^1 Bq/ $\mu\text{Ah/g-MoO}_3$ at $t = 0$ and 24 h. In Table 2, we show these yield

Table 2 Radioactivities produced from the bremsstrahlung γ -ray beam irradiation of 3 min on a 1 g $^{nat}\text{MoO}_3$ target using a 30 MeV electron beam with a 1 μA intensity

Nucleus	Half-life	Activity ($t = 0$)	Activity ($t = 24$ h)
		Bq/ $\mu\text{Ah/g-MoO}_3$	Bq/ $\mu\text{Ah/g-MoO}_3$
^{90}Mo	5.7 h	$(1.7 \pm 0.1) \times 10^3$	$(9.0 \pm 0.5) \times 10^1$
^{90}Nb	14.6 h	$(1.7 \pm 0.1) \times 10^3$	$(1.3 \pm 0.2) \times 10^1$
^{91m}Nb	61 days	≤ 80	≤ 80
^{91}Mo	15.5 m	Not determined	Not determined
^{92m}Nb	10.2 days	$(7.7 \pm 0.9) \times 10^1$	$(7.2 \pm 0.9) \times 10^1$
^{95}Nb	35 days	$(2.1 \pm 0.3) \times 10^2$	$(2.7 \pm 0.3) \times 10^2$
^{95m}Nb	3.6 days	$(4.5 \pm 0.4) \times 10^2$	$(3.7 \pm 0.3) \times 10^3$
^{96}Nb	23 h	$(1.08 \pm 0.04) \times 10^4$	$(5.2 \pm 0.1) \times 10^2$
^{97}Nb	72 m	$(3.9 \pm 0.4) \times 10^5$	$(3.2 \pm 0.4) \times 10^{-1}$
^{98m}Nb	51 m	$(2.5 \pm 0.5) \times 10^3$	$(7.9 \pm 1.6) \times 10^{-6}$
^{99}Mo	66 h	$(1.05 \pm 0.06) \times 10^5$	$(8.1 \pm 0.4) \times 10^4$
^{99m}Tc	6 h	$(1.1 \pm 0.1) \times 10^4$	$(7.4 \pm 0.9) \times 10^4$

values which would be useful for the impurity estimation of ^{91m}Nb in extraction of ^{99m}Tc .

- The decay curve of 511 keV γ -rays are well fitted with a half-life of $T_{1/2} = 15.5$ m for the ^{91}Mo β^+ decay only at the elapsed time less than 4 h. However, the amount of radioactivities has not been reliably determined at $t = 0$ because of high background in the γ -ray spectra at the short elapsed times. Since the spin-parity of the ^{91}Mo ground state with $T_{1/2} = 15.5$ m is $9/2^+$, the direct excitation strength via the $^{92}\text{Mo}(\gamma, n) ^{91}\text{Mo}$ ($J^\pi = 9/2^+$) reaction is expected to be small. On the other hand, the spin-parity of the 653 keV first excited state in ^{91}Mo is $J^\pi = 1/2^-$ and this state decays with a very short half-life of $T_{1/2} = 65$ s by β^+ decay. Therefore, this situation also makes it very difficult to determine the amount of the ^{91}Mo radioactivity at $t = 0$.
- The 934 keV peak was identified to be due to the ^{92m}Nb decay. Since the ^{92m}Nb half-life is long as $T_{1/2} = 10.2$ days and the background level of the γ -ray spectra soon after the beam irradiation is high, we could not reliably obtain the radioactivity yields at $t = 0$. Although the error bar is relatively large, we give the yield estimations as $(7.7 \pm 0.9) \times 10^1$ Bq/ $\mu\text{Ah/g-MoO}_3$ at $t = 0$, and is $(7.2 \pm 0.9) \times 10^1$ Bq/ $\mu\text{Ah/g-MoO}_3$ at $t = 24$ h.

Kikunaga reported the experimental result for the ^{99}Mo production from bremsstrahlung γ -rays using the 40 MeV electron linear accelerator at Tohoku University in Japan [25]. He concluded that 3000 Bq of ^{99}Mo radioactivities could be obtained when an enriched ^{100}Mo target with a thickness of 1 mg/cm² was bombarded for a 1-h irradiation time with 1 μA . His result leads to the estimation that about 600 GBq of ^{99}Mo production is realized with 20 h

irradiation by using a 1 mA 40 MeV electron-beam and a 10 g ^{100}Mo metal-target. A similar result was obtained at $E_\gamma = 30$ MeV in the simulation calculations by Starovoitova et al. [26]. Recently, Tadokoro of Hitachi Co. Ltd estimates the ^{99}Mo production using the Monte-Carlo radiation transport calculation code PHITS [27]. He concludes that the ^{99}Mo production is expected to reach at 1340 GBq using a 35 MeV electron beam with a current of 1 mA for 20 h irradiation on the 100% enriched ^{100}Mo target [28]. These facts give us a convincing argument that when we irradiate the 1 mA electron beam on a $^{nat}\text{MoO}_3$ target with a thickness of 10 g/cm² and with a diameter of 2 cm for 20 h, the produced ^{99}Mo activity amounts to 120 GBq. If we take into account the abundance of ^{100}Mo in ^{nat}Mo , 0.0963 and this value is corrected for, we obtain a value of 1246 GBq, which is roughly in agreement with the Tadokoro's result of 1340 GBq obtained with a 100% enriched ^{100}Mo target.

However, it should be noted that the aforementioned value for the ^{99}Mo production is obtained under the assumption that a 100% enriched ^{100}Mo target is placed at the position close to a thin platinum (Pt) target. This is not realistic because a high-intensity electron beam after penetrating the Pt target will directly enter into the Mo target, and will induce a huge heat-deposit inside of the Mo target, leading to the thermo-fusion of the target.

Figure 6 shows the simulation for the energy distribution of out-coming electrons when a 30 MeV electron beam passes through the Pt target with a thickness of 0.4 cm. This calculation was made by using the code G4beamline [22]. As imaged by looking at the shape of the bremsstrahlung γ -ray spectrum (see also Fig. 1), electrons generating high-energy γ -rays lose most of their energies, and electrons generating low-energy γ -rays lose a small part of their energies, resulting a widely spread energy

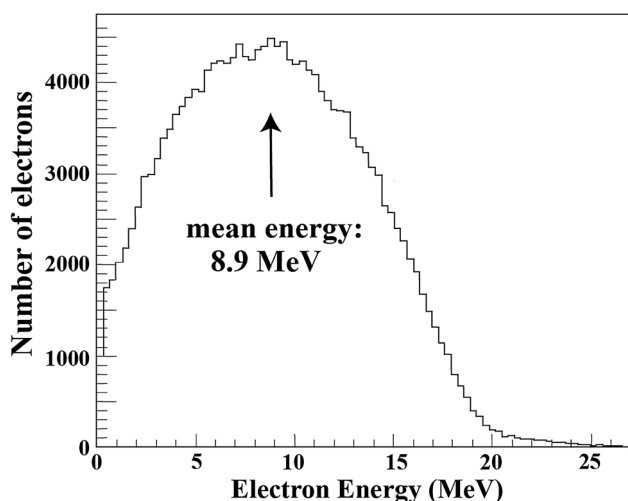


Fig. 6 Simulated energy distribution of out-coming electrons when a 30 MeV energy electron beam penetrates the bremsstrahlung Pt target with a thickness of 0.4 cm. The number of in-coming 30 MeV electrons is assumed to be 10^7 in total. The electron beam is assumed to bombard the Pt target with a spot size of 1 cm diameter. The distance between the Pt target and the Mo target entrance is assumed to be 1 cm. Out-coming electrons of about 1.8×10^5 pass through the area with a diameter of 0.8 cm. The ratio of out-coming to in-coming electrons is $1.8 \times 10^5/10^7 = 1.8 \times 10^{-2}$. It is noted that most electrons hitting the Pt target are not scattered at forward angles, and spread by scattering over the outside of the target area

distribution of out-coming electrons from the Pt target. The mean energy of energy-lost electrons is 8.9 MeV, and the maximum energy is about 20 MeV, although there is a small tail over the region above 20 MeV. If a 1 mA electron beam bombards the Pt target, and a MoO₃ target with diameter of 2 cm and with a length of 5 cm is used, the energy deposit due to out-coming electrons inside of the MoO₃ target amounts to about 1 kW, leading to the melting of MoO₃ powders in the target capsule. This causes serious difficulties in the next chemical process for extracting ^{99m}Tc. Therefore, we cannot set a MoO₃ target just behind the Pt target without any good instrumental idea. It is essential to insert a strong magnetic field between the Pt target and the Mo target for avoiding the direct electron beam irradiation. This problem would be solved by using a compact-size permanent magnet.

The relation between the magnetic field $B(\text{T})$ and the orbital radius $r(\text{m})$ of an electron is given as follows;

$$r(\text{m}) = 3.33 \times \frac{p(\text{GeV}/c)}{B(\text{T})}, \quad (2)$$

where the electron momentum $p(\text{GeV}/c)$ is nearly equal to $E(\text{GeV}/c)$. Taking into account that the energy of out-coming electrons passing through the bremsstrahlung target with a thickness of 0.4 cm are about 20 MeV at maximum, we need to bend these electrons away from the ^{nat}MoO₃ target. This is feasible by putting a permanent magnet with

strength of 1 T and with a gap of 3 cm. The 20 MeV electron beam after passing through the Pt target is bent with an orbit radius of 6.6 cm. Thus, it is rather easy to put the Mo target at a 10 cm backward position from the Pt target, and to insert a magnet with strength of 1 T and with a length of 8 cm between them to avoid the heat deposit due to the direct bombardment of the electron beam.

On base of the experimental result presented in Table 2, we can estimate the amount of the ^{99m}Tc radioactivity under the following conditions:

1. The ^{nat}MoO₃ powder with a standard density of 4.69 g/cm³ is packed into the cylinder capsule with a diameter of 2 cm and with a length of 5 cm. The total weight of ^{nat}MoO₃ becomes 74 g.
2. A permanent magnet with strength of 1 T and a length of 8 cm is inserted between the Pt target, and the cylinder capsule is put along the γ -ray beam axis.
3. The distance from the Pt target and the front end of the cylinder is 10 cm.
4. The target is irradiated for 20 h with the bremsstrahlung γ -rays generated with a 1 mA electron beam at 30 MeV.
5. Since we increase the target density, it is necessary to estimate the γ -ray attenuation of 0.39, which is given using the equation for γ -ray attenuation in matter, $P(x) = \exp(-\mu/\rho \cdot x)$, where $x = 5 \times 4.69 \text{ g/cm}^2$ and the photon mass attenuation coefficient $\mu/\rho = 0.04 \text{ cm}^2/\text{g}$ for 30 MeV γ -rays, which is given in Ref. [29]. Note that the density of ^{nat}MoO₃ powder is 4.69 g/cm³.

Taking into account all the conditions mentioned above, we obtain 6.6 GBq of ^{99m}Tc radioactivity at the elapsed time of 24 h after 20 h irradiation with a 1 mA 30 MeV electron beam. The ^{99m}Tc milking may take place 5 times a week. Considering this situation, the amount of ^{99m}Tc radioactivities reaches at $6.6 \times 2.5 = 16.5 \text{ GBq}$. The factor of 2.5 comes from the sum of $0.777 + 0.604 + 0.469 + 0.365 + 0.283$, where five numerical numbers are due to the decay of ⁹⁹Mo with $T_{1/2} = 66 \text{ h}$ in step of each milking. Since 0.3 GBq is used for each SECT inspection, we can produce ^{99m}Tc pharmaceuticals for 55 patients from the daily operation of the electron linear accelerator.

In case of Japan, for example, it has been reported that about 2000 TBq of ⁹⁹Mo activity is imported every year for 106 SPECT inspections. Since 2000 TBq divided by 10^6 is equal to 2 GBq, we arrive at the conclusion that 2 GBq is consumed for each SPECT inspection on an average. Therefore, the total usage efficiency of ⁹⁹Mo becomes to be $0.3 \text{ GBq}/2 \text{ GBq} \sim 1/6$. About 5/6 of the ⁹⁹Mo isotopes imported from abroad disappears without being used in case of Japan. The main part of this disappearance is due to

the decay of the radioactivities, and the other part would be due to the poor efficiency of the radioactivity treatment.

Taking into account the extraction efficiency and the decay loss from ^{99}Mo to $^{99\text{m}}\text{Tc}$, and also the decay loss during the ^{99}Mo overseas transportation from abroad, this 1/6 usage efficiency reduction seems to be reasonable. If the usage efficiency of ^{99}Mo is 1/6, Japan only needs to produce $2000/6 = 333$ TBq for one million SPECT inspections. If a 1 mA electron linear accelerator can be operated for 20 h a day and 200 days a year, the produced $^{99\text{m}}\text{Tc}$ activities support $55 \times 200 = 11,000$ SPECT inspections. This means that Japan needs to have about 100 electron accelerators. At present, there are about 150 PET cyclotrons for producing ^{18}F -FDG in Japan. Thus, a large number of 100 electron accelerators in one country are not surprising. It is possible to reduce this number of 100 electron accelerators by reducing the distance between the Pt target and the Mo target in order to increase the $^{99\text{m}}\text{Tc}$ production rate. It is also possible to reduce the number of accelerators if the electron beam current is vastly increased. Apparently, if enriched ^{100}Mo target is used, it is feasible to reduce the number of accelerators to about 1/10 although another problem happens in connection with a high cost of enriched ^{100}Mo and its sustainability.

Considering the countermeasures against a surge in price rise of ^{99}Mo medical isotopes due to the molybdenum crisis [4], the cost reduction by applying $^{\text{nat}}\text{Mo}(\gamma, n)$ reaction for the ^{99}Mo generation becomes essential. Since the half-life of $^{99\text{m}}\text{Tc}$ is 6 h, the delivery system of $^{99\text{m}}\text{Tc}$ pharmaceuticals will be most-likely established as those for ^{18}F ($T_{1/2} = 2$ h) for a local area. The direct $^{99\text{m}}\text{Tc}$ delivery system would be established by car transportation within a 200–300 km circle area from an accelerator facility since delivery services will be accomplished within 6 h. In addition, it would be possible for us to use airplane transportation to deliver $^{99\text{m}}\text{Tc}$ pharmaceuticals for local towns or for neighboring countries, if necessary.

The remaining problem is whether $^{99\text{m}}\text{Tc}$ radioactivities are separately extracted among the impurity Nb and Mo radioisotopes produced via the photoreactions. An important issue is to satisfy the USP (U.S. Pharmacopeia) compounding standard [19] condition, which requires the produced $^{99\text{m}}\text{Tc}$ pharmaceuticals to keep impurities less than 0.01% of $^{99\text{m}}\text{Tc}$. As shown in Table 2, we have experimentally confirmed the fact that the produced radioactivities are mostly due to the Nb and Mo isotopes, and $^{99\text{m}}\text{Tc}$ isotopes are only obtained from the β^- decay of ^{99}Mo .

There are two methods: the one is by the solvent extraction method, and the other by the sublimation method. The solvent extraction methods are reviewed by Molinski [30] and Noronha [31] in detail. Recently, Nakai et al. [16] have showed a solvent-extraction method with

MEK (methyl ethyl ketone) with a compact chemical apparatus named “Tc generator” [32], which enables us to overcome the aforementioned difficulties in extracting pure $^{99\text{m}}\text{Tc}$ isotopes with low specific activities of Nb and Mo for satisfying the USP condition. One concern of chemical problems is the expenses for treatment of waste disposals in the chemical process. To relieve this concern, a sustainable system should be established by recycling the used $^{\text{nat}}\text{Mo}$ powder. Starovoitova et al., [26] propose to use nano-particle of molybdenum. If the Mo (γ, n) reaction happens in Mo metallic powders with a size of 20–30 nm, recoiled high-energy ions like ^{99}Mo escape from the surface of nano-particles, and stop at an interstice among nano-particles. Using proper chemical liquids like MEK, only the $^{99\text{m}}\text{Tc}$ radioactivities can be resolved and extracted from molybdenum nano-particles. In this case, it is needed for filtering out nano-particles in the used chemical liquid. Nowadays, porous sintered metals of molybdenum are technically feasible. Usage of such porous sintered metals could be one way to wash out only produced $^{99\text{m}}\text{Tc}$ radioactivities while leaving Nb and Mo radioactivities in the sintered metal.

Another way is a sublimation method. The solvent extraction methods are purely based on the chemical technique. On the other hand, in the sublimation method, $^{99\text{m}}\text{Tc}$ is extracted by using the temperature difference of evaporation among Nb, Mo and Tc on base of the property differences in physical compounds (see Ref. [33] and references therein). A concern has been still remained: When the MoO_3 powder is heated up, the crystallization proceeds with increasing temperature and the grain size increases by a factor of about 10. This grain size increase may cause deterioration of the sublimation efficiency of KTcO_4 . Further examination of the proposed sustainable system is needed for making $^{99\text{m}}\text{Tc}$ radio-pharmaceuticals. Both the aforementioned methods are still needed for further technological development in realizing a new sustainable $^{99\text{m}}\text{Tc}$ supply system.

Final remarks and conclusion

$^{99\text{m}}\text{Tc}$ isotopes with $T_{1/2} = 6$ h are used for the SPECT inspections for health-care diagnosis. $^{99\text{m}}\text{Tc}$ isotopes are extracted by the milking method from ^{99}Mo isotopes with $T_{1/2} = 66$ h. The long half-life of ^{99}Mo gives a great merit to allow us to make overseas transportation with international flights.

The ^{99}Mo isotopes are produced as a fission product from ^{235}U in a limited number of research nuclear reactors, most of which now encounter the problem in stable operation due to aging long after their construction, and due to the expiration of the reactor usage [4]. The supply price of

^{99}Mo isotopes has been cheap for a long time, because the major part of operation cost of research nuclear reactors is mostly supported by a huge government budget, and the radioactivity production division is a small part compared with the total operational cost of such research nuclear reactors. Taking into consideration the balance sheet between the ^{99}Mo production and its operation costs, the price of ^{99}Mo isotopes could be expected to be significantly high in near future. This makes a big cost mismatch compared with those of the positron emission tomography (PET) inspection, in which ^{18}F isotopes are commercially produced without any government support.

High cost problem will happen when we use enriched ^{100}Mo isotopes for producing ^{99}Mo via the $^{100}\text{Mo}(\gamma, n)$ reaction. Since enriched ^{100}Mo isotopes are artificially produced using a centrifugal separator in a limited number of countries, another associated problem will happen from the viewpoint of the sustainable supply of $^{99}\text{Mo}/^{99\text{m}}\text{Tc}$ isotopes to receiver hospitals.

We studied the feasibility of the $^{99\text{m}}\text{Tc}$ production via photoreactions on $^{\text{nat}}\text{MoO}_3$ at electron accelerator facilities. Instead of the usage of proton and neutron induced reactions, it is not necessary to use enriched ^{100}Mo isotopes. This becomes a great merit for cost reduction. We have discussed the sustained availability of $^{99\text{m}}\text{Tc}$ isotopes via the $^{\text{nat}}\text{Mo}(\gamma, n)$ reaction. For this purpose, we have measured the radioactivities yielded via photoreactions on $^{\text{nat}}\text{MoO}_3$ with bremsstrahlung γ -rays. As expected, various Nb and Mo isotopes are found to be produced. It should be noted here that Tc isotopes other than $^{99\text{m}}\text{Tc}$ are not produced in case of the photoreaction with the $^{\text{nat}}\text{MoO}_3$ target. Therefore, using the differences of chemical or physical properties among $^{99\text{m}}\text{Tc}$, Mo and Nb, the produced $^{99\text{m}}\text{Tc}$ isotopes are separated from other residual isotopes in the solvent extraction methods or the sublimation method even if the impurity ratios of Mo and Nb is high. We have quantitatively obtained the amounts of observed radioactivities in normalized unit of $\text{Bq}/\mu\text{Ah}/\text{g}\text{-MoO}_3$. These measured results contribute to solve the technical problems for extracting pure $^{99\text{m}}\text{Tc}$ isotopes separated from other Mo and Nb impurities for estimating contamination impurities which should be less than 10^{-4} to satisfy the specification requirement of the United States Pharmacopeial Convention [19].

Several subjects of further investigation still remain for realistic construction of the electron accelerator facilities providing a high intensity beam with an inexpensive cost. The number of such facilities could be compatible with those of the PET cyclotron facilities to satisfy the self-sufficiency of $^{99}\text{Mo}/^{99\text{m}}\text{Tc}$ isotopes, reducing a high barrier for construction and operation of research nuclear reactors and enriched ^{100}Mo production facilities. In addition, it is necessary for us to optimize the irradiation system of

bremsstrahlung γ -rays in combination with the electron-beam sweep magnet, the cooling system of the Pt target, the mounting device of $^{\text{nat}}\text{MoO}_3$ powder targets, and the extraction system of $^{99\text{m}}\text{Tc}$ isotopes.

Acknowledgements The authors thank T. Nagae and K. Nakai for their encouragement during the development of the present work. They also thank M. Nishimura and Y. Aiba of Kyocera Co. Ltd. for discussion. The present experiment was performed at the electron linear accelerator facility of the Institute for Integrated Radiation and Nuclear Science, Kyoto University (KURNS) under a user program (Proposal No. 29137). This work was supported in part by Grants-in-Aid for Scientific Research in Japan (Grant No. 15H02091).

References

1. Perrier C, Segre E (1937) Technetium: the element of atomic number 43. *J Chem Phys* 5:712–716
2. Perrier C, Segre E (1937) Technetium: radioactive isotopes of element 43. *Nature* 140:193–194
3. Richards P, Tucker WD, Srivastava SC (1982) Technetium-99 m: an historical perspective. *Int J Appl Radiat Isot* 33:793–799
4. Van Noorden RM (2013) The medical testing crisis. *Nature* 504:202–204
5. Disarmament and Related Treaties (PTBT). https://issuu.com/unpublications/docs/disarmament_and_related_treaties. Accessed 5 Mar 2001
6. Treaty on the Non-Proliferation of Nuclear Weapons (NPT). <https://www.un.org/disarmament/wmd/nuclear/npt/>. Accessed 5 Mar 2018
7. Graham A (2010) Nuclear terrorism fact sheet. belfer center for science and international affairs. Harvard Kennedy School. <https://belfercenter.org/publication/nuclear-terrorism-fact-sheet.html>. Accessed 5 Mar 2018
8. National Academies of Sciences, Engineering, and Medicine (2016) Molybdenum-99 for medical imaging. The National Academies Press, Washington. <https://www.nap.edu/catalog/23563/molybdenum-99-for-medical-imaging>. Accessed 5 Mar 2018
9. Sholten B, Lambrecht RM, Cogneau M, Ruiz HV, Qaim SM (1999) Excitation functions for the cyclotron production of $^{99\text{m}}\text{Tc}$ and ^{99}Mo . *Appl Radiat Isot* 51:69–80
10. Nagai Y, Hatsukawa Y (2009) Production of ^{99}Mo for nuclear medicine by $^{100}\text{Mo}(n,2n)^{99}\text{Mo}$. *J Phys Soc Jpn* 78:033201
11. Gue'rin B, Tremblay S, Rodrigue S, Rousseau JA, Dumulon-Perreault V, Lecomte Van Lier, Van Lier RE, Zyuzin A, Van Lier AE (2010) Cyclotron production of $^{99\text{m}}\text{Tc}$: an approach to the medical isotope crisis. *J Nucl Med* 51:13N–16N
12. Lyra M (2011) Alternative production methods to face global molybdenum-99 supply shortage. *Hell J Nucl Med* 14:49–55
13. Jalilian AR, Targholizadeh H, Raisali GR, Zandi H, Kamali Dehgan M (2011) Direct technetium radio-pharmaceuticals production using a 30 MeV cyclotron. *DARU J Pharmaceut Sci* 19:187–192
14. Pillai MRA, Dash A, Knapp FF (2013) Sustained availability of $^{99\text{m}}\text{Tc}$: possible paths forward. *J Nucl Med* 54:313–323
15. Qaim SM, Sudar S, Scholten B, Koning AJ, Coenen HH (2014) Evaluation of excitation functions of $^{100}\text{Mo}(p, d + pn)^{99}\text{Mo}$ and $^{100}\text{Mo}(p, 2n)^{99\text{m}}\text{Tc}$ reactions: estimation of long-lived Tc-impurity and its implication on the specific activity of cyclotron-produced $^{99\text{m}}\text{Tc}$. *Appl Radiat Isot* 85:101–113

16. Nakai K, Takahashi N, Hatazawa J, Shinozuka A, Hayashi Y, Ikeda H, Kanai Y, Watabe T, Fukuda M, Hatanaka K (2014) Feasibility studies towards future self-sufficient supply of the ^{99}Mo – $^{99\text{m}}\text{Tc}$ isotopes with Japanese accelerators. *Proc Jpn Acad B90*: 413–420. <https://www.ncbi.nlm.nih.gov/pmc/articles/PMC4335138/>. Accessed 5 Mar 2018
17. Tkac P, Vandergrift GF (2016) Recycle of enriched Mo targets for economic production of $^{99}\text{Mo}/^{99\text{m}}\text{Tc}$ medical isotope without use of enriched uranium. *J Radioanal Nucl Chem* 308:205–212
18. Morley TJ, Dodd M, Gagnon K, Hanemaayer V, Wilson J, McQuarrie SA, English W, Ruth TJ, Benard F, Schaffer P (2012) An automated module for the separation and purification of cyclotron-produced $^{99\text{m}}\text{TcO}_4^-$. *Nucl Med Biol* 39:551–559
19. General Chapter < 979 >Pharmaceutical compounding—sterile preparations. <http://www.usp.org/compounding/general-chapter-797>. Accessed 5 Mar 2018
20. Institute for Integrated Radiation and Nuclear Science, Kyoto University: Electron Linear Accelerator. <http://www.rri.kyoto-u.ac.jp/en/facilities/ela>. Accessed 27 July 2018
21. Mang'era K, Ogbomo K, Zriba R, Fitzpatrick J, Brown J, Pellerin E, Barnard J, Saunders C, De Jong M (2015) Processing and evaluation of linear accelerator-produced $^{99}\text{Mo}/^{99\text{m}}\text{Tc}$ in Canada. *J Radioanal Nucl Chem* 305:79–85
22. G4beamline (2018). <http://muonsinternal.com/muons3/G4beamline>. Accessed 5 Mar 2018
23. Geant4 (2018). <http://geant4.cern.ch>. Accessed 5 Mar 2018
24. Beil H, Berg'ere R, Carlos R, Lepretre A, De Miniac A, Veysiere A (1974) A Study of the photoneutron contribution to the giant dipole resonance in doubly even Mo isotopes. *Nucl Phys A* 227:427–449
25. Kikunaga H (2015) RI production via photonuclear reaction with electron linear accelerator (in Japanese). http://www.rcnp.osaka-u.ac.jp/medsci/MedSciSympo2015/Presentation/part2/MedSciKickoffSympo2015_Part2_Kikunaga.pdf. Accessed 5 Mar 2018
26. Starovoitova VN, Tchelidze L, Wells DP (2014) Production of medical radioisotopes with linear accelerator. *Appl Radiat Isot* 85:39–44
27. Particle and Heavy ion transport code system (PHITS). <https://phits.jaea.go.jp/index.html>. Accessed 5 Mar 2018
28. Tadokoro T (2017) Production of medical radioactive nuclides using an electron linear accelerator (in Program of 2017 Symposium on Nuclear Data November 16–17, 2017). <http://www.aesj.or.jp/ndd/symposium2017/programme.html>. Accessed 5 Mar 2018
29. Greeniaus LG (1987) TRIUMF kinematics handbook
30. Molinski VJ (1982) A review of $^{99\text{m}}\text{Tc}$ generator technology. *Int J Appl Radiat Isot* 33:811–819
31. Noronha OPD, Seuatkar AB (1983) Solvent extraction technology of ^{99}Mo – $^{99\text{m}}\text{Tc}$ generator system 1: an indian experience: progress design and operational considerations. <https://doi.org/10.1080/10256018608623597>. Accessed 5 Mar 2018
32. Takahashi N (2014) RI isolation device: patent 2014/057900A1 (international). <https://patents.google.com/patent/WO2014057900A1/en>. Accessed 5 Mar 2018
33. Fujiwara M, Nakai K, Takahashi N, Hayakawa T, Shizuma T, Miyamoto S, Fan GT, Takemoto A, Yamaguchi M, Nishimura M (2017) Production of medical $^{99\text{m}}\text{Tc}$ isotopes via photonuclear reaction. *Phys Part Nucl* 48:124–133